INTERNATIONAL JOURNAL FOR NUMERICAL AND ANALYTICAL METHODS IN GEOMECHANICS
Int. J. Numer. Anal. Meth. Geomech. (2007)
Published online in Wiley InterScience (www.interscience.wiley.com). DOI: 10.1002/nag.656

A discrete element model for kaolinite aggregate formation during sedimentation

Ning Lu[1,*,†,‡,§], Matthew T. Anderson[1], William J. Likos[2,¶] and Graham W. Mustoe[1]

[1]*Engineering Division, Colorado School of Mines, Golden, CO 80401, U.S.A.*
[2]*Department of Civil and Environmental Engineering, University of Missouri, Columbia, MO 65211, U.S.A.*

SUMMARY

The formation of colloidal aggregates during sedimentation is an important process when considering geotechnical and environmental engineering problems including wastewater treatment systems and slurry wall constructions for waste isolation. In this paper, a quasi three-dimensional discrete element framework is developed to model aggregate formation during sedimentation by considering the following microscopic inter-particle forces present in the clay–water–electrolyte system: van der Waals attraction, electrical double-layer repulsion, Born's repulsion, hydrodynamic viscous drag, and gravity. The role of these physico-chemical forces in the formation of clay clusters during sedimentation is investigated using an integrated numerical and experimental approach. The discrete element method (DEM) framework has been previously shown to accurately model clay behavior at the microscopic level. The model is validated with experimental data for comparison of distributions of aggregate density and aggregate size. Good agreement between the model prediction and the experimental results is obtained, suggesting that the DEM can be a powerful tool to better understand the aggregate formation process at the microscopic scale. For particle sizes ranging from 0.05 to 1 μm it is also shown, through numerical simulations, that ionic strength of the fluid medium is the controlling factor for aggregate size and density and that at aggregate sizes less than 20 μm, face-to-face interactions dominate the force regime between a pair of particles. Copyright © 2007 John Wiley & Sons, Ltd.

Received 21 February 2006; Revised 25 January 2007; Accepted 20 June 2007

KEY WORDS: discrete elements; clay behavior; sedimentation; granular media; clay–water–electrolyte

*Correspondence to: Ning Lu, Engineering Division, Colorado School of Mines, Golden, CO 80401, U.S.A.
†E-mail: ninglu@mines.edu
‡Professor.
§Former Graduate Student.
¶Assistant Professor.

INTRODUCTION

Many environmental and geotechnical engineering problems involve the formation of colloidal aggregates during sedimentation. Practical examples include the design of wastewater treatment systems and construction of slurry walls for waste isolation. The performance of these engineered systems depends heavily on our understanding of how colloidal aggregates form and on their controlling parameters during flocculation. Aggregate properties such as density and size have a direct impact on their engineering performance. For example, the sedimentation rate of colloidal aggregates in a waste treatment facility depends on aggregate size and aggregate density. It is also well known in geotechnical and environmental engineering that the density and size of clay aggregates have a strong impact on macroscopic hydrological and mechanical properties of soils such as soil permeability, strength, and deformation [1–3].

This study is concerned with the formation of kaolinite aggregates in electrolyte solutions, specifically examining the effects that control aggregate size and density. Because clay particles are typically very small in size (e.g. $<1\,\mu m$) and large in specific surface (e.g. 15–20 m^2/g for kaolinite), physico-chemical forces dominate the particle interactions in suspension and the resulting sedimentation behavior. Accordingly, aggregate size and density are controlled by the magnitude of these physico-chemical forces.

Discrete particle groups, or aggregates, are formed when a balance is reached between all the forces experienced by the particles settling in the solution. These forces include attractive inter-particle forces, repulsive inter-particle forces, gravitational forces, and hydrodynamic forces. Forces tending to aggregate the particles include short-range van der Waals attraction and edge-to-face electrical double-layer interaction. Forces tending to disperse the particles include face-to-face double-layer interaction and sedimentation-induced fluid shear.

Double-layer interaction forces, whether attractive or repulsive, are a direct function of solution properties and the charge density of the clay particle surface. The van der Waals attraction is a function of clay mineralogy and the dielectric constant of the clay–water–electrolyte system, described by the Hamaker constant [4].

Understanding the size and density of aggregates formed during sedimentation has been an intensive subject in environmental engineering and water resources research. A previous study by Tambo and Wantanabe [5] suggests that as aggregate size increases, the densities approach a constant value. Recent work by Likos and Lu [6] using a laser sizing technique confirms the earlier observation for aggregate sizes ranging from 1 to 6 μm. For aggregate sizes from 25 to 125 μm, it has been shown that there exists a power-law relationship between aggregate density and size [7].

Both experimental and theoretical studies exist in this area but they are far from sufficient for the many emerging geotechnical and environmental problems, such as clay liners for waste containment and compaction of expansive soils. For the most part, previous experimental studies employed optical techniques at scales greater than microns. At present, non-destructive and direct observations at sub-micron scale are either not available or inaccurate. Theoretical studies have focused mainly on individual particle interactions. Direct quantitative simulation of group behavior such as distributions of particle size and density is still lacking.

In this study, a discrete element framework is employed to directly simulate the sedimentation process of an assembly of colloidal clay particles in suspension. This discrete element method (DEM) framework has recently been shown to accurately model clay behavior at the microscopic level [8, 9]. The formation of aggregates is simulated by considering all the important physico-chemical forces and hydrodynamic forces acting on each kaolinite particle. Parameters including

DOI: 10.1002/nag

particle size, surface charge density, double-layer thickness, and Hamaker constant are selected to be representative of kaolinite clay particles. The model is validated against experimental data from Likos and Lu [6] by comparing distributions of aggregate density and size.

CONCEPTUAL AGGREGATE MODEL AND EXPERIMENTAL EVIDENCE

When considering fine-grained soils, it is known that soil fabric is the fundamental governing parameter for permeability (e.g. Casagrande [10]; Mitchell [11]; Lambe and Whitman [12]; Collins and McGown [13]). It has been shown experimentally [1–3] that physico-chemical variables, which govern the soil fabric, including pore-fluid chemistry and clay mineralogy will greatly affect the mechanical and hydrological properties of fine-grained soils. Olsen [14] explained this phenomenon with the development of the cluster model, which conceptualizes that the soil fabric is governed by physico-chemical forces.

Clay aggregate formation occurs when the physico-chemical and mechanical forces in a colloidal system are in equilibrium. The formation process described here is the simplified conceptual model shown in Figure 1. Aggregates are formed as a result of the force balance between van der Waals and edge-to-face attractions, and electrical double-layer repulsion. The attractive forces tend to

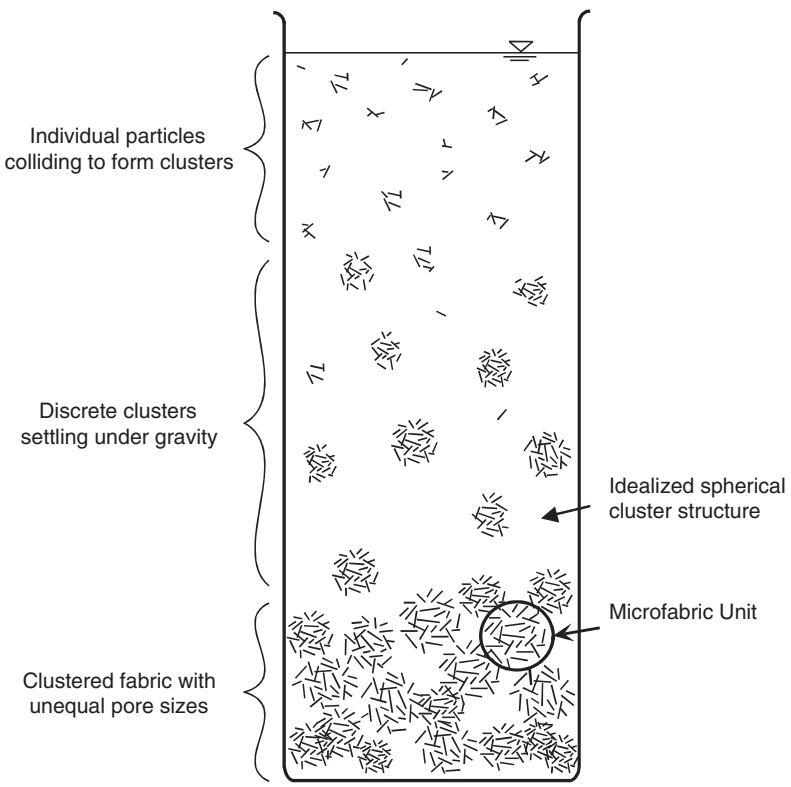

Figure 1. Conceptual model for the formation of kaolinite aggregates during sedimentation.

DOI: 10.1002/nag

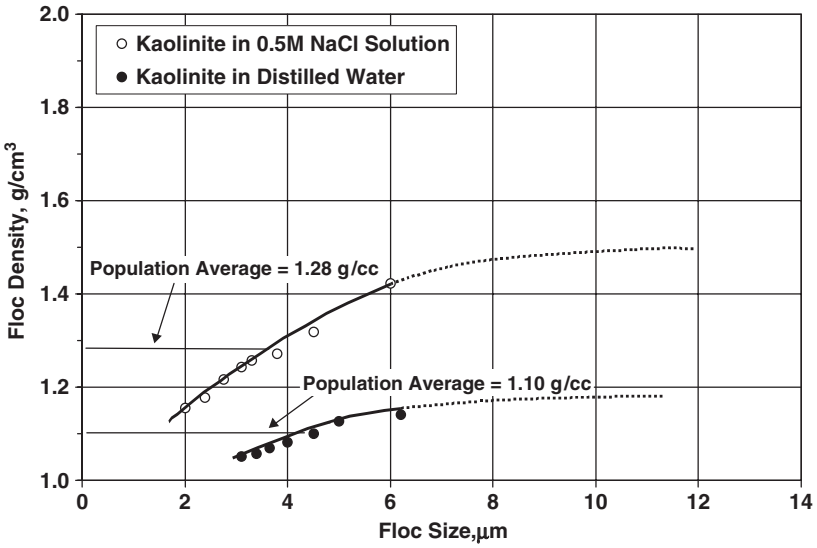

Figure 2. Aggregate density as a function of size and ionic strength (after Likos and Lu [6]). The dashed lines are projections based on conceptualization and previous understanding.

flocculate or aggregate particles, while the repulsive force disperse the particles. Differential settling of a range of particle sizes brings the individual particles into close proximity and eventually contact. If the energy from the particle contact allows stabilization of the net force between the particles, they will flocculate and form successively larger aggregates. As particles settle, aggregate size eventually reaches a maximum when the hydrodynamic viscous drag force reaches equilibrium with the physico-chemical attractive/repulsive and mechanical forces acting on the particle as it settles in a fluid [15].

At this stage of the sedimentation process, the porosity of the aggregate is a strong function of the electrical double-layer thickness. When the thickness of the double layer increases, it is more difficult for the opposing forces to reach equilibrium and the tendency for particles to flocculate decreases; this is illustrated in Figure 2 for aggregate sizes of <10 μm for Georgia kaolinite particles. The dashed lines in Figure 2 are the extrapolations of the aggregate densities for reference purpose, since our experimental technique does not yield statistically confident results for an aggregate size greater than 10 μm. Nevertheless, some previous studies (e.g. Li and Ganczarzyk [16]) showed that there exists an asymptotic aggregate density for a given ionic strength. The electrical double-layer thickness is controlled by clay mineralogy and the properties of the fluid medium which includes the dielectric constant, solute concentration, surface charge, cation valence, and the temperature (e.g. Rosen [17]; Van Olphen [18]).

THEORETICAL FORMULATION

Interactions between small soil particles, dissolved ions, and water are caused by unbalanced force fields at the interfaces between soil and water. When two particles are in close proximity, their

DOI: 10.1002/nag

respective force fields overlap and influence the behavior of the system. Clay particles, because of their very small sizes and platy shapes, have large surface areas and are especially influenced by these forces.

The effects of surface force interactions and small particle sizes are manifested by a variety of inter-particle attractive and repulsive forces, which, in turn, influence the flocculation behavior of clays in suspension, volume change characteristics, and strength properties of clays at common void ratios. Because the fabric of a clay at the time of formation may have a profound influence on its engineering properties, insight into the factors that influence the flocculation behavior is of considerable value.

To better describe the microscopic behavior of clays, the following microscopic forces are explicitly considered in the discrete element simulation. They are the electrical double-layer repulsion, van der Waals attraction, hydrodynamic viscous drag, and Born's repulsion.

Electrical double-layer repulsive force (*physico-chemical*)

The mixed double layer has been widely considered in geotechnical engineering (e.g. Bolt [1]; Mitchell [19]), and is accounted for here. In dry clay, adsorbed cations are tightly held by the negatively charged clay particles. Cations in excess of those needed to neutralize the electronegativity of the clay particles and associated anions are present as salt precipitates. When the clay is placed in water, the precipitated salts go into solution. Because the adsorbed cations produce a much higher concentration near the surfaces of the particles, they try to diffuse away in order to equalize concentrations throughout. Their freedom to do so, however, is restricted by the negative electrical field originating at the particle surfaces. The escaping tendency due to diffusion and the opposing electrostatic attraction leads to ion distributions adjacent to clay particles in suspension. The charged surface and the distributed charge in the adjacent phase are together termed as the electrical double layer (e.g. Van Olphen [4]).

The controlling variables for the magnitude of the electrical double-layer repulsive force are illustrated in Figure 3, where the electrical double-layer repulsion is portrayed as a function of the thickness of the electrical double layer $1/\kappa$ and the inter-particle distance d.

For two spherical particles of radii r_1 and r_2, surface potentials ψ_1 and ψ_2, and a surface-to-surface distance d, the repulsive force is [20]

$$U(d) = \frac{\pi\varepsilon r_1 r_2(\psi_1^2 + \psi_2^2)}{r_1 + r_2} \left\{ \frac{2\psi_1\psi_2}{\psi_1^2 + \psi_2^2} \ln \frac{1 + \exp(-\kappa d)}{1 - \exp(-\kappa d)} - \ln[1 - \exp(-2\kappa d)] \right\} \tag{1}$$

where κ is the inverse of the double-layer thickness and ε is equal to $\varepsilon_0 * D$, where D is the dielectric constant and ε_0 the permittivity of the vacuum.

van der Waals attractive force (*physico-chemical*)

Since clay particles are highly polar materials and their faces carry a negative bulk charge, attraction will result due to the induced dipole effect. For an assembly of colloidal particles, attractive forces are additive and the van der Waals interaction energy between particles can be computed by summing the attractions between all inter-particle pairs (e.g. Russel *et al.* [21]; Shaw [22]). Figure 3 shows the nature of the van der Waals attractive force as a function of the Hamaker constant for different clay minerals and the inter-particle distance.

DOI: 10.1002/nag

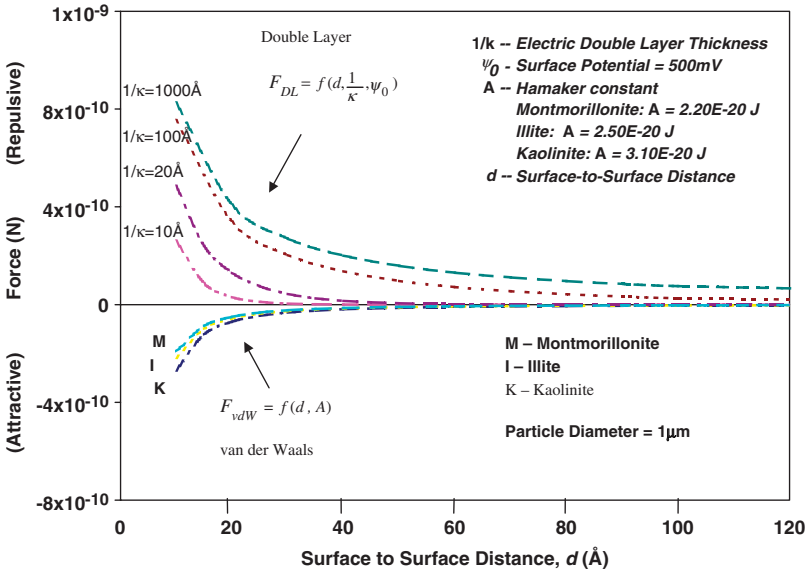

Figure 3. Nature of physico-chemical forces between two adjacent particles in a clay–water–electrolyte system: electrical double-layer repulsion as a function of surface potential, particle separation distance, the double-layer thickness, and the particle radii; and the van der Waals attraction as a function of clay mineralogy, particle separation distance, and particle radii (from Anderson and Lu [9]).

According to Chen and Anandarajah [23], the van der Waals attractive force includes a non-retarded contribution and a retarded contribution. For simplicity, the non-retarded force is considered here. For two spherical particles of radii r_1 and r_2, and a surface-to-surface distance d, the attractive force is

$$F(d) = A\frac{r_1 + r_2 + d}{3}\left[\begin{array}{l} -\dfrac{1}{d(d+2r_1+2r_2)} + \dfrac{1}{(d+r_1)(d+r_2)} \\ +\dfrac{2r_1r_2}{d^2(d+2r_1+2r_2)^2} + \dfrac{2r_1r_2}{(d+r_1)^2(d+r_2)^2} \end{array}\right] \tag{2}$$

where A is the Hamaker constant having an approximate value of 10^{-20} J for clay minerals (e.g. Lyklema [24]).

Hydrodynamic viscous drag force (*mechanical*)

Hydrodynamic viscous drag is considered in this study because it is important during the process of sedimentation, swelling, and colloid transport in porous media. The viscous drag is often described by Stokes law, which depicts the force as a function of fluid viscosity, particle diameter, and particle velocity.

Our previous study [8] showed that without considering the viscous force, the gravitational force dominated the system and did not allow the physico-chemical forces to act in a proper manner to yield realistic predictions of settling velocity. To counteract this phenomenon, a drag force was

DOI: 10.1002/nag

added to model clay particles settling in a fluid. According to Stokes [25], the translational drag resistance for spherical particles is

$$c_i = 3\pi D \tag{3}$$

where D is the diameter of the sphere, and subscript i indicates the principal directions of x and y in a two-dimensional space [26]. The viscous drag can be expressed as

$$F_i = -\mu c_i v_i \tag{4}$$

where μ is the viscosity, and v_i the velocity components in the principal directions. The resultant drag forces in the horizontal and vertical directions are as follows [27]:

$$\begin{aligned} F_x &= -3\mu\pi D v_x \\ F_y &= -3\mu\pi D v_y \end{aligned} \tag{5}$$

By combining Equations (3)–(5), together with weight, and buoyancy forces, the well-known velocity estimation for spherical particles can be obtained

$$v = \frac{2(G_s - G_f)}{9\mu}\left(\frac{D}{2}\right)^2 \tag{6}$$

where G_s is the specific gravity of solid and G_f is the specific gravity of fluid. The settling velocity for other shapes can also be obtained analytically following the same approach [27].

Born's repulsion (mechanical)

The mechanical contact forces are usually characterized in a DEM algorithm with elastic, inelastic, and frictional behavior (e.g. Cundall and Strack [28]; Mustoe [29]; Williams and Mustoe [30]; Thomas and Bray [15]). It is important to recognize that the normal elastic resistance described above originates from Born's repulsion, which is the inter-atomic resistance. In other words, as two molecules approach each other very closely and the outer electron shells start to overlap, strong electrostatic repulsion occurs. Because outer electrons of one molecule are forbidden to enter occupied orbitals of another, this leads to repulsion, increasing steeply with decreasing inter-particle distance. This phenomenon is called 'hard core' or 'Born's' repulsion [24].

No generally valid law exists for this repulsion. The most popular methods of modeling this include exponential functions, power laws, and steep linear relations [24]. Here, Born's repulsive force is considered as a steep linear function that acts at an inter-particle distance of up to 6 Å (e.g. Ryan and Elimelech [31]). Consequently, in the region of 0–6 Å the repulsive force will dominate and will be very similar to the traditional treatment of the mechanical contact force in DEMs (e.g. Cundall and Strack [28]).

Net inter-particle force system

The complex nature of the net force regime acting between two spherical particles due to the presence of physico-chemical forces is illustrated in Figure 4. In general, there are three force domains. When two particles are far away from each other there is a net repulsive force depending on the parameters of the clay and the pore fluid. The range of the electrical double-layer repulsive force, as shown in this example, is greater than 10 Å but less than 50 Å with a peak value at

DOI: 10.1002/nag

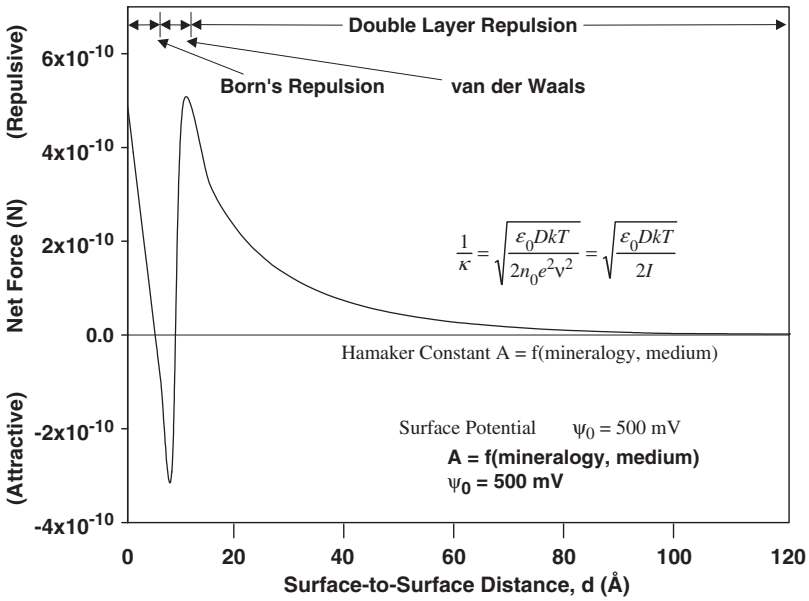

Figure 4. An illustration of the complex nature of the net force between two adjacent particles with the following parameters: the particle diameter is 1 μm, the thickness of the double layer $1/\kappa$ is 50 Å, the surface potential ψ_0 of the clay particles is 500 mV, and the Hamaker constant A for the particle–water–particle system is 2.2E−20 J.

a distance of 15 Å. When the distance between the particles is in the range of 6–10 Å, the van der Waals attraction dominates. The maximum attractive force occurs at about 8 Å. At very small inter-particle distances, from 0 to 6 Å, Born' repulsion dominates. This is the so-called contact force that prevents the two particles from penetrating into each other.

The van der Waals attractive force regime illustrated here to be in the range of 6–10 Å is considered to be the source of cohesion, whereas the electrical double-layer repulsive regime is responsible for soil swelling and dispersion among clay particles. Both van der Waals attractive and electrical double-layer repulsive forces are strongly pronounced in cohesive soils. In this study, the role of these two physico-chemical forces in the formation of clay clusters during sedimentation is investigated using an integrated numerical and experimental approach.

DISCRETE ELEMENT IMPLEMENTATION

The DEM is based on an explicit time-stepping numerical scheme in which the interaction of the particles is monitored contact by contact and the motion of the particles is modeled particle by particle. The contact forces and motions of an assembly of disc-shaped particles are found through a series of calculations tracing the motions of individual particles. These motions are a result of the propagation through the medium of disturbances originating at the boundaries and such propagation is a dynamic process. The speed of the propagation is primarily a function of the pore medium (i.e. pore fluid).

DOI: 10.1002/nag

In describing the above dynamic behavior numerically, a series of time-stepping calculations are performed. Note, within each time step calculation the particle accelerations are assumed to be constant. Because of the use of the explicit time-stepping scheme in the DEM, the time step is chosen so small that during a single step disturbances from any particle cannot propagate further than its immediate neighbors. At each successive time step, the resultant forces on any particle are determined exclusively by its interaction with neighboring particles that are either in contact or in the region where the electrical double layer and van der Waals forces are acting. It is the simplicity of the DEM algorithm, which makes it possible to model the complex non-linear interactions within an assemblage containing a large number of particles without excessive memory requirements or the need for an iterative procedure [32].

The calculations performed in the DEM alternate between the application of Newton's second law to all the particles and Newton's third law, which is used in combination with the particle–particle interaction forces for every pair of interacting particles. Newton's second law determines the acceleration of a particle resulting from the forces acting on it. From this information, a simple velocity and position update for each particle is performed.

The deformations of the individual particles are considered to be small in comparison with the deformation of an assembly of particles as a whole. The latter deformation is primarily due to the rigid body motions of the individual particles. Therefore, precise modeling of particle deformation is not necessary in order to obtain a good approximation of the mechanical behavior.

The forces, including both mechanical and physico-chemical forces, acting on a particle are computed and summed. These forces in turn are used to find new accelerations using Newton's second law. These accelerations are assumed to be constant over the time step and can be integrated to obtain the velocity and finally the new position of the particle.

This cycle is repeated again and again: the forces corresponding to the displacements are found using the force–displacement law and the force sums, including physico-chemical forces, and are substituted into Newton's second law to obtain displacements.

Particle generation and selection of an appropriate time step are very important in the framework. All of the simulations have spherical particles with different size distributions generated for the initial particle distribution. For unambiguous comparison, particles with different diameters are initially uniformly positioned in a two-dimensional rectangular domain.

A small time step is chosen so that each particle can only interact with its nearest neighbors. This ensures that the resultant forces, physico-chemical and mechanical, are determined solely by the particles whose force fields overlap.

SIMULATION RESULTS

The DEM framework investigates the size and density of kaolinite aggregates formed during sedimentation under the influence of solutions of differing ionic strength and differing surface electric potential. Ionic strength is defined as (e.g. Langmuir [33])

$$I = \sum \frac{1}{2} n v^2 \tag{7}$$

where n is the absolute chemical concentration and v is the valence of the ion. The surface charge is a characteristic of the clay mineral type.

DOI: 10.1002/nag

Table I. Pertinent parameters with which all DEM simulations are run for Georgia kaolinite.

Clay type	Hamaker constant, A (J)	Particle size range (μm)	Surface potential, ψ (mV)	Cation valence, v	Specific surface area (m^2/g)	Solution concentration (mol)
Georgia kaolinite	3.1×10^{-20}	0.5–2.0	50–250	1	20	0.001–1.0

All the DEM simulations are run with discrete particle groups, uniformly positioned, containing about 700 particles. The particles range in diameter from 0.05 to 1.0 μm based on the values from previous experiments [6]. The electrolyte concentration of the solution varies from 0.001 to 1.0 M and the surface charge varies from 50 to 250 mV, which is a common range for kaolinite [34]. Each of the simulations is specified to run for 7000 ms or 7 s, long enough to ensure that flocculation occurs and allows equilibrium to occur within each of the discrete particle groups.

All numerical simulations are run with parameters representative of Georgia kaolinite as shown in Table I. Probability distributions were generated for each of the simulations and the majority of the aggregate sizes are in the 2–14 μm range, less than 10% of the population of aggregates fell outside this range.

The DEM framework presents data for each of the 700 particles considered in the simulation. The data include size, location, and mass as well as settling velocity. Aggregate size and density are calculated by fitting a sphere around each aggregate as shown in Figure 1. Aggregates are treated as separate clusters if the closest distance between the adjacent particles is less than 10 Å. By idealizing the aggregates as spheres and having data for each particle, it is possible to approximately calculate the size (diameter) and the density of each aggregate.

The time evolution of kaolinite aggregate formation during sedimentation in an assembly of colloidal clay particles under the influence of van der Waals attraction, electrical double-layer repulsion, Born's repulsion, hydrodynamic viscous drag, and gravity is presented in Figure 5. Figure 5(a) depicts the aggregate formation under the influence of an electrolyte solution of 0.001 M, a relatively low ionic strength. Figure 5(b) and (c) shows the aggregate formation under concentrations of 0.1 M (a medium to high ionic strength) and 1.0 M (a high ionic strength), respectively. In all the three series of simulations (a)–(c), the initial positions of particles are the same. With a concentration of low ionic strength, the electrical double-layer force is dominant and the tendency of particles to flocculate is less likely. As the ionic strength of the solution increases, the ability of the opposing attractive forces to overcome the electrical double-layer force becomes more likely and the maximum density is asymptotically approached at a cluster size of 10 μm (see also Figure 2). Finally, at high ionic strength, almost all of the particles will flocculate and settle at a much higher velocity but as the aggregate size approaches 15 μm, the density of the aggregates begins to decrease. By comparing Figure 5(a)–(c), it can be observed that the difference in the cluster formations between Figure 5(a) ($I = 0$) and Figure 5(b) and (c) ($I = 0.1$ and 1 M) is much larger than the difference between Figure 5(b) and (c).

Impact of ionic strength on aggregate density and size

Figure 6 illustrates the calculated aggregate density as a function of the aggregate size and the ionic strength of the solution. The results in Figure 6 depict a similar trend of the effect of ionic strength on the aggregate size and aggregate density compared with the experimental results (also shown in Figure 2). The aggregate density reaches a maximum at a floc size of about 8–10 μm

DOI: 10.1002/nag

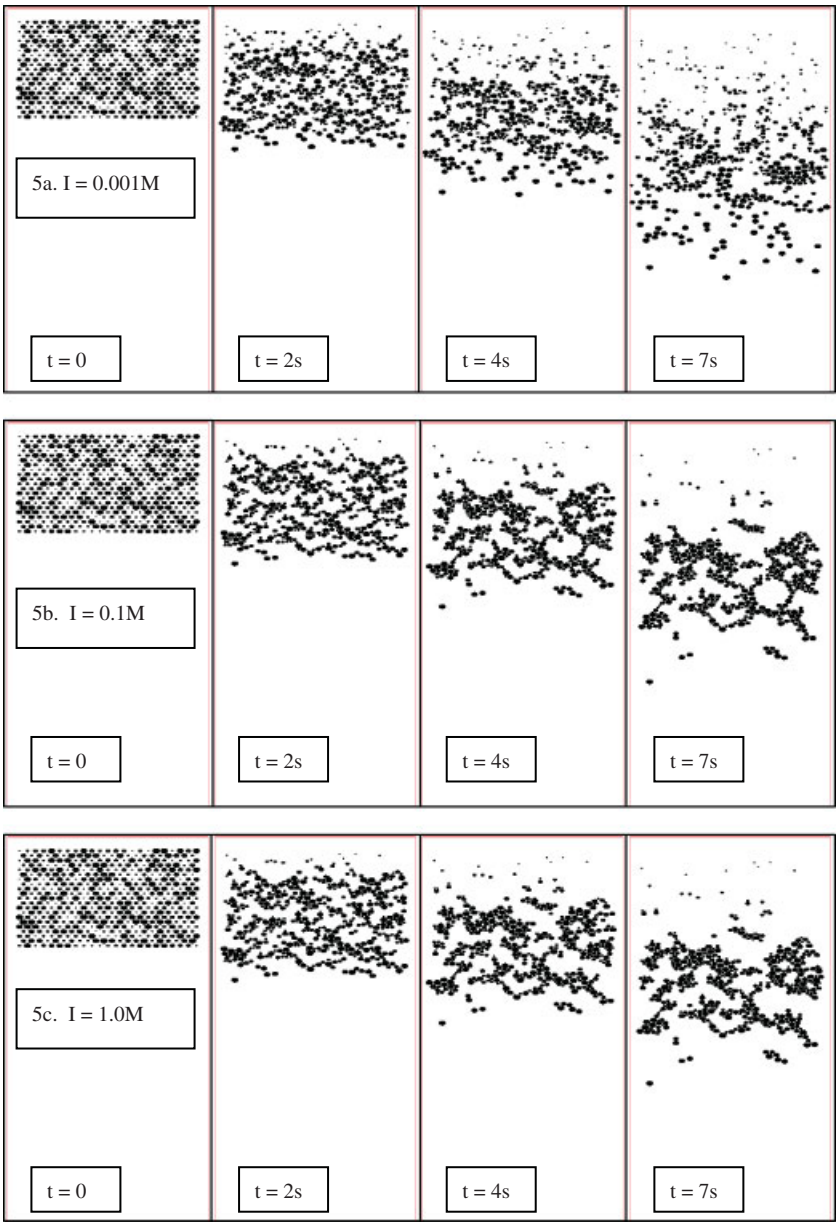

Figure 5. DEM simulation of the sedimentation of kaolinite under the influence of physico-chemical forces: (a) low ionic strength; (b) medium ionic strength; and (c) high ionic strength.

for all the three values of ionic strength. When the aggregate size exceeds this value, the density begins to slowly decrease. These trends are consistent with experimental results obtained using laser diffraction by Likos and Lu [6].

DOI: 10.1002/nag

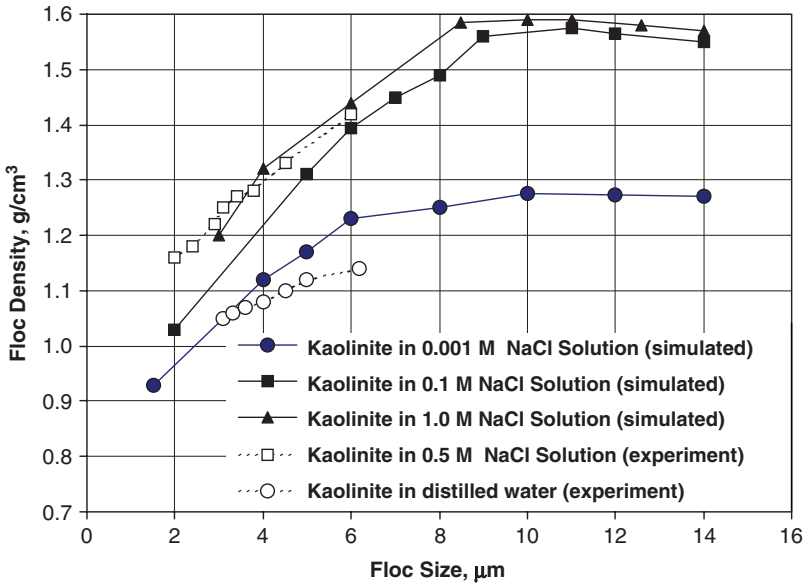

Figure 6. The effect of ionic strength on aggregate density and size.

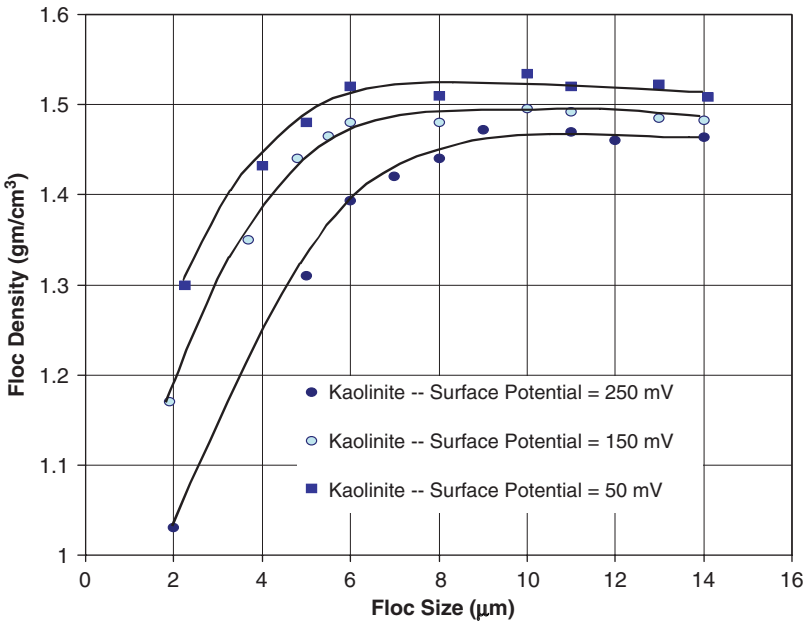

Figure 7. The effect of surface potential on aggregate density and size. The curves are the best fitting for the simulated results shown in symbols.

DOI: 10.1002/nag

There exists some discrepancy in aggregate density between the experimental and numerical results, this is most likely because of the shape of the particles used in the simulations. Kaolinite particles are platy shaped, but are simulated in the DEM algorithm as discs due to computational limitations. Previous works by others (e.g. see the edited volume by Williams and Mustoe [30]) indicate that particle shapes are important in many mechanical behaviors of granular media. This approximation may lead to a higher volume than that of platy particles. Because of this difference, the density of the aggregates are continually overestimated in the DEM simulations but the trend between the DEM and experimental data is similar.

Impact of surface charge on aggregate density and size

Figure 7 illustrates the effect of varying surface charge on the aggregate size and aggregate density of a colloidal system of kaolinite particles. The trends evident in Figure 7 are qualitatively consistent with double-layer theory [19, 34]; as the surface charge decreases, the double-layer thickness decreases and the density of the kaolinite aggregates increases. Based on these simulations, it is observed that the effect of the surface charge, however, is not as pronounced as that of the ionic strength with respect to aggregate size and density. For example, as the surface charge decreases from 250 to 50 mV, the maximum density of the aggregates increases from 1.47 to 1.53 g/cm^3. On the other hand, as the ionic strength increases from 0.001 to 1.0 M, the maximum density increases from 1.275 to 1.59 g/cm^3 (Figure 7).

DISCUSSION

The aggregate size and aggregate density trends present in the DEM simulations for solutions of differing ionic strength are qualitatively consistent with experimental evidence and double-layer theory. As the electrolyte concentration of the solution increases, the electrical double layer collapses. As the double layer collapses, the repulsive force between individual particles decreases and the tendency for those particles to flocculate increases. With a decrease in the repulsive forces and an increase in flocculation in the clay–water–electrolyte system, the fabric of individual aggregates becomes less porous and an increase in density is observed. This is consistent with the experimental evidence obtained by Kuroda *et al.* [35] for kaolinite aggregates in NaCl solutions ranging from 0.03 to 0.5 M using photographic techniques for quantifying aggregate sizes.

Experimental studies have been performed for aggregates formed with a variety of materials including bentonite and alum aggregates (e.g. Matsumoto and Mori [36]), activated sludge [5, 16, 37], quartz [38], and marine sediment [39]. These previous studies show that the density decreases as aggregate size increases for aggregate sizes larger than approximately 25 μm and the relationship between aggregate density and size was consistent with power-law relationships. However, there is some uncertainty involved in the above data because of the definition of clusters.

Our numerical study shows that as aggregate size increases, the aggregate density also increases for a range of aggregate sizes from 2 to 10 μm. As aggregate size becomes larger than 10 μm, a slight decrease becomes apparent in the density of the aggregates for solutions of higher ionic strength; this is consistent with several other studies of larger aggregate sizes (e.g. Tambo and Watanabe [5]). These numerical results are comparable with experimental results obtained by Likos and Lu [6] who used a laser particle counter to measure aggregate density and size. Their results showed that as aggregate size increases from 1 to 6 μm, there is an increase in aggregate

DOI: 10.1002/nag

density. However, there is no sufficient data for aggregate sizes over 6 μm. Figure 5 also illustrates the effect that aggregate size has on the settling velocity of particles immersed in solution. Our simulation results also demonstrate that as the sizes of the aggregates and the settling velocity increase, the amount of particles at the top of the sedimentation column decreases.

The scale of the aggregates that are investigated can explain the discrepancy between the previously mentioned experimental work and this study. In this study, the size of aggregates investigated is in the range of 2–14 μm. At this scale, the soil fabric is dominated by face-to-face interactions between particles including electrical double-layer repulsion and van der Waals attraction (e.g. Mitchell [34]). As the size of the aggregate increases from the tens of microns range to the hundreds of micron range, edge-to-face attractions are likely to be the dominating mechanisms for the soil fabric. The edge-to-face interactions add a degree of porosity to the aggregates thereby increasing the size; this may account for the inconsistency in the results, as these edge-to-face interactions are not considered in this numerical study.

SUMMARY AND CONCLUSIONS

A DEM framework is developed and employed to quantitatively model the formation of kaolinite aggregates during the sedimentation process. Inter-particle forces of the electrical double-layer repulsion, van der Waals attraction, and Born's repulsion are considered in the DEM formulation. Hydrodynamic viscous drag is also considered. Born's repulsion is the basis for the normal contact force between two contacting particles.

The simulation results for the sedimentation tests are compared with the experimental results obtained using a laser particle counter [6]. Sensitivity simulations were also conducted to determine the effect of ionic strength and surface charge on aggregate size and aggregate density. The following conclusions can be drawn from this study:

(1) The numerical simulations predicted similar trends when compared with the experimental data. The numerical simulations slightly overestimated the density of the aggregates for the entire range of aggregate sizes and electrolyte concentrations. However, there was only a difference of about 10% when comparing the experimental and numerical data. These similar trends validate the hypothesis that for small aggregate sizes, 2–14 μm, face-to-face interactions dominate the force regime between two particles.
(2) The implementation of the microscopic physico-chemical forces for clay particles demonstrates that the DEM can be an effective tool for studying the flocculation behavior of clay particles in solutions of differing ionic strengths.
(3) The sensitivity simulations show that ionic strength has a substantially more profound effect on the flocculation behavior of clays when compared with that of the surface charge. As the surface charge increases from 50 to 250 mV, the density of the aggregates increases by a modest 9%. However, when the concentration of the solution increases from 0.001 to 1.0 M which is commonly encountered in geotechnical and environmental engineering, the density of the aggregates increases by 25%. Also, as the ionic strength the increases, the aggregate density asymptotically approaches a maximum around 1.60 g/cm^3, which is confirmed by some previous experimental studies.
(4) The difference between the experimental and numerical results can be attributed mainly to the fact that in this study, the clay particles are modeled as spheres and not as platy-shaped

DOI: 10.1002/nag

particles, which are much more indicative of the real shape. Other physical mechanisms and computational limitations may have also caused these differences such as the number of particles. Examples of other physical mechanisms are clay hydration and edge-to-face attractions, both of which occur in clays.

Future work in this area will have to include the ability to specify non-circular-shaped particles and the ability to use significantly more particles in each of the simulations to better represent the formation of aggregates during sedimentation. Some recent works by others demonstrate that the DEM simulation of granular media with various shapes and large number of particles is possible with the current computational capabilities. Physical and chemical heterogeneties in the formation of clay aggregates may also be incorporated to reflect the reality. Current computational limitations exist when attempting to model a representative elementary volume of particles that is smaller than 1 mm. Finally, the hydrodynamic viscous drag forces could be better simulated by some detailed fluid–solid interaction models.

REFERENCES

1. Bolt GH. Physico-chemical analysis of the compressibility of pure clays. *Geotechnique* 1956; **6**(2):86–93.
2. Olsen HW. Hydraulic flow through saturated clays. *Proceedings of the 9th National Conference on Clays and Clay Minerals*. Pergaman Press: West Lafayette, IN, 1962; 131–161.
3. Mesri G, Olson RE. Mechanisms controlling the permeability of clays. *Clays and Clay Minerals* 1971; **19**:151–158.
4. Van Olphen H. *Clay Colloid Chemistry* (2nd edn). Krieger Publishing Company: Malabar, FL, 1991.
5. Tambo N, Watanabe Y. Physical characteristics of flocs—I. The floc density function and aluminum floc. *Water Resources* 1979; **13**:409–419.
6. Likos WJ, Lu N. A laser technique to quantify the size, porosity, and density of clay clusters under sedimentation conditions. *Geotechnical Testing Journal* (ASTM) 2001; **24**(1):86–94.
7. Gibbs RJ. Settling velocity, diameter, and density for flocs of illite, kaolinite, and montmorillonite. *Journal of Sedimentary Petrology* 1985; **55**(1):65–68.
8. Anderson MT, Lu N, Mustoe GGM. A discrete element simulation of the forming of clay aggregates during sedimentation. *Proceedings of the 20th ASCE Engineering Mechanics Conference*, Austin, TX, 2000.
9. Anderson MT, Lu N. The role of microscopic physico-chemical forces in the large volumetric strains for clay sediments. *Journal of Engineering Mechanics* (ASCE) 2001; **127**:710–719.
10. Casagrande A. The structure of clay and its importance in foundation engineering. *Contributions to Soil Mechanics, 1925–1940*. Boston Society of Civil Engineers: Boston, 1932; 71–112.
11. Mitchell JK. The fabric of natural clays and its relation to engineering properties. *Proceedings of the Highway Research Board* 1956; **35**:693–713.
12. Lambe TW, Whitman RV. *Soil Mechanics*. Wiley: New York, 1969.
13. Collins K, McGown A. The form and function of microfabric features in a variety of natural soils. *Geotechnique* 1974; **24**.
14. Olsen HW. Hydraulic flow through saturated clays. *ScD. Dissertation*, MIT, MA, 1961.
15. Thomas PA, Bray J. Capturing nonspherical shape of granular media with disk clusters. *Journal of Geotechnical and Geoenvironmental Engineering* 1999; **125**:169–178.
16. Li DH, Ganczarzyk JJ. Stroboscopic determination of settling velocity, size, and porosity of activated sludge flocs. *Water Resources* 1987; **23**(3):257–262.
17. Rosen MJ. *Surfactants and Interfacial Phenomena* (2nd edn). Wiley: New York, 1989; 431.
18. Van Olphen H. *An Introduction to Clay Colloid Chemistry*. Krieger Publishing Company: Malabar, FL, 1991.
19. Mitchell JK. *Fundamentals of Soil Behaviour* (2nd edn). Wiley, 1991.
20. Hogg R, Healy TW, Fuerstenau DW. *Transactions of the Faraday Society* 1966; **62**:1638.
21. Russel WB, Saville DA, Schowalter WR. *Colloidal Dispersions*. Cambridge University Press: Cambridge, 1989; 525.
22. Shaw DJ. *Introduction to Surface and Colloid Chemistry* (4th edn). Butterworth-Heinemann: London, 1992.
23. Chen J, Anandarajah A. van der Waals attraction between spherical particles. *Journal of Colloid and Interface Science* 1996; **168**:111–117.

DOI: 10.1002/nag

24. Lyklema J. *Fundamentals of Interface and Colloid Science*: *Volume 2*. Academic Press: New York, 1991.
25. Stokes GG. *Transactions of the Cambridge Philosophical Society* 1851; **9**:8–27.
26. Clift R, Grace JR, Weber ME. *Bubbles*, *Drops*, *and Particles*. Academic Press: New York, 1978; 380.
27. Lu N, Ristow G, Likos WJ. Accuracy of hydrometer analysis for fine-grained clay particles. *Geotechnical Testing Journal* (ASTM) 2000; **23**(4):487–495.
28. Cundall PA, Strack ODL. In *Modeling of Microscopic Mechanisms in Granular Media*: *New Models and Constitutive Relations*, Jenkins JT, Satake M (eds). Elsevier: Amsterdam, 1983; 137–150.
29. Mustoe GGW. A generalized formulation of the discrete element method. *Engineering Computations* 1992; **9**(2):181–190.
30. Williams JR, Mustoe GGW (eds). *Proceedings of the 2nd International Conference on Discrete Element Methods*. MIT Press: Boston, MA, 1993.
31. Ryan JN, Elimelech M. Colloid mobilization and transport in groundwater. *Colloids and Surfaces* 1976; **107**:1–56.
32. Cundall PA, Strack ODL. A distinct element method for modeling granular assemblies. *Geotechnique* 1979; **29**:47–65.
33. Langmuir D. *Environmental Aqueous Geochemistry*. Prentice-Hall: Englewood Cliffs, NJ, 1997.
34. Mitchell JK. *Fundamentals of Soil Behavior* (2nd edn). Wiley: New York, 1993.
35. Kuroda Y, Nakaishi K, Shirata R. The interface of salt concentration on structure of kaolinite floc. *Journal of the Clay Science Society of Japan* 1998; **37**(4):137–143.
36. Matsumoto K, Mori Y. Settling velocity of flocs—new measurement method of floc density. *Journal of Chemical Engineers of Japan* 1975; **8**(2):143–147.
37. Magara Y, Hambu S, Utosawa K. Biochemical and physical properties of activated sludge on settling characteristics. *Water Resources* 1976; **10**:71–77.
38. Klimpel RC, Hogg R. Effects of flocculation conditions on agglomerate structure. *Journal of Colloid and Interface Science* 1986; **113**(1):121–131.
39. McCave IN. Vertical fluxes of particles in the ocean. *Deep Sea Resources* 1992; **22**:491–502.

DOI: 10.1002/nag